

Status of leptoquark models after LHC Run-2 and discovery prospects at future colliders

Nishita Desai*

*Department of Theoretical Physics,
Tata Institute of Fundamental Research,
Mumbai, India 400005*

Amartya Sengupta

Meghnad Saha Pally, Burdwan, India, 713104 †

We study limits from dilepton searches on leptoquark completions to the Standard Model in the parameter space motivated by anomalies in the $b \rightarrow s$ sector. After a full Run-2 analysis by LHCb, the disparity in lepton flavour violation has disappeared. However, the mismatch in angular distributions as well as in $B_s \rightarrow \mu^+ \mu^-$ partial width is still unresolved and still implies a possible new physics contribution. We probe three models of leptoquarks — scalar models S_3 and R_2 as well as vector leptoquark model U_1 using non-resonant dilepton searches to place limit on both the mass and couplings to SM fermions. The exclusions of leptoquarks coupling either non-uniformly to different lepton flavours or uniformly is examined. Interestingly, if leptoquark couplings to electrons and muons are indeed universal, then the U_1 model parameter space that corresponds to the anomalous contribution should already accessible with Run-2 data in the non-resonant $e\mu$ channel. In the non-universal case, there is a significant exclusion in couplings, but not enough to reach regions that explain observed anomalies. We, therefore, examine the prospective sensitivity at the HL-LHC as well as of a 3 TeV future muon collider. For the vector leptoquark model, we find that a muon collider can probe all of the relevant parameter space at 95% confidence with just 1 fb^{-1} data whereas R_2 and S_3 models can be excluded at 95% with 5 fb^{-1} and 6.5 fb^{-1} luminosity respectively.

* nishita.desai@tifr.res.in

† amartya.sengupta@studenti.unipd.it

I. INTRODUCTION

An exciting development in recent years has been the measurement of ratios of decay widths in the semileptonic rare decays of B-mesons [1–4], hinting at lepton flavour-universality violation (LFV). The latest of these [1, 2] showed a measurement consistent with the SM for certain lepton universality, however, there remains a mismatch with the measured branching fraction of $B_s \rightarrow \mu^+\mu^-$ [3, 4] and in the angular distribution in the decay $B \rightarrow K^*\mu^+\mu^-$ [5, 6]. Unsurprisingly, this has led to a spirited effort to understand the source of the mismatch with the predictions of the Standard Model (SM) and to provide new physics explanations for it. In particular, there have been several dedicated studies that determine global fits to data in terms of effective field theoretic operators (see e.g. [7–11]). There has also been some effort to explain the anomalies in terms of new particles, notably with new vector bosons or leptoquarks [12–15]. The effects of the presence of such new particles can generally be seen in other observables besides the LFV ratios, and in particular, in the high energy tails of certain distributions observable at the LHC. In this paper, we examine the expected effects of leptoquarks with minimally required properties to cause observed anomalies in the B-sector and report on current constraints and future prospects of their detection.

We start by providing a bare-bones introduction to how the Effective Field Theoretic (EFT) framework is used and translated to the measurement of the high-energy observables that we examine in this paper. EFT provides a useful method to describe the low-energy physics processes in which the short-distance (i.e. high-energy or UV) physics is encapsulated in the Wilson coefficients whilst the rest of the long-distance physics is expressed in terms of effective operators with those having dimensions higher than four being suppressed by powers of an energy scale to maintain the mass dimension of each term in the Lagrangian. The analytic form of the Wilson coefficient can then be calculated by “matching” the expressions calculated from the EFT with the expressions from the full UV theory. We can use the published value by one of the multiple groups to translate the B-meson observations into best-fit values of the appropriate Wilson coefficients [7–11, 16]. We then match these values to the expressions derived from the leptoquark model under study and study the consequence of what that means on other production mechanisms at the LHC.

The anomalies seen in the data fall into two categories — (1) in the neutral current sector

with $b \rightarrow s$ transitions, and (2) in the charged current sector with $b \rightarrow c$ transitions. In this work, we concentrate mainly on models that explain the first of these [17], however, it is known that one of the models we study viz. the U_1 vector leptoquark can explain both simultaneously (see e.g. table 2. of [12])

The relevant observations that motivate this work based on the full Run 1 and 2 dataset are shown in table II in the appendix. For completeness, we show both the pre-December 2022 LHCb announcement [1, 2] numbers, as well as the latest measurements.

The low-energy effective theory for the $b \rightarrow s$ flavour changing neutral current sector is described in terms of an effective Hamiltonian which can be written as

$$\mathcal{H}_{\text{eff}} = -\frac{4G_F}{\sqrt{2}}V_{tb}V_{ts}^* \left\{ \sum \mathcal{C}_i(\mu)\mathcal{O}_i(\mu) \right\}$$

where $\mathcal{C}_i(\mu)$ are the Wilson coefficients. The effective operators relevant to our study are

$$\mathcal{O}_9^{l_1 l_2} = \frac{e^2}{(4\pi)^2}(\bar{s}\gamma_\mu P_L b)(\bar{l}_1\gamma^\mu l_2), \quad \mathcal{O}_{10}^{l_1 l_2} = \frac{e^2}{(4\pi)^2}(\bar{s}\gamma_\mu P_L b)(\bar{l}_1\gamma^\mu\gamma^5 l_2) \quad (\text{I.1})$$

Multiple fitting studies have found that the operator whose Wilson coefficient shows significant deviation from the predicted SM value is the C_9 and that the most likely discrepancy seems to be in the $C_9^{\mu^+\mu^-}$ coefficient. To stay consistent with the latest data, we use the

Author (Year)	Model Dependent	Data Driven
Ciuchini et al (2022) [7]	$[-1.25, -0.72]$	$[-1.10, 1.05]$
Ciuchini et al (2019) [8]	$[-1.37, -1.05]$	$[-1.47, -0.93]$
Algueró et al (2019) [9]	$[-1.15, -0.81]$	
Alok et al (2019) [10]	$[-1.27, -0.91]$	
Mahmoudi et al (2021) [11]	$[-1.07, -0.83]$	

TABLE I. Best Fit values for the new physics contribution to the operator C_9 . The first of these contains the updated 2022 results. The fits taking into account angular distributions still favour a similar range as before the 2022 LHCb data release even though the overall best fit 1σ range is now consistent with the SM value of zero.

most recent best-fit results as reported in [7]. We shall use the best fit values that correctly give the angular correlations as well (the so called “model-dependent” fit). However, later in the paper when we examine future prospects, we also show the overlap with the fully agnostic data-driven fits. For an overview of the best-fit C_9 values see table I. Currently, we proceed by using the value

$$C_9^{\mu^+\mu^-} = -0.98 \pm 0.27,$$

Multiple studies have also examined the leptoquark UV completion and calculated explicit expressions for $C_9^{\mu^+\mu^-}$ from each model. In this work, we use these expressions to investigate the LHC constraints on the couplings and mass of the leptoquarks. We make only the minimal assumptions, i.e. only the couplings that are necessary to give a contribution to the $b \rightarrow s$ anomalies is assumed to be non-zero. As we shall see, in each leptoquark model, the Wilson coefficients $C_{9(10)}$ depend on three parameters roughly as

$$C_9 \sim \left(\frac{y_{22} y_{32}}{M} \right)^2$$

where y_{22} is the $s\mu$ coupling, y_{32} is the $b\mu$ coupling and M is the mass of the leptoquark. We start by constraining (y_{22}, y_{32}, M) in other production modes without any further assumptions on other leptoquark couplings. This results in the most conservative limits. In the case where there is no LFV, one would expect identical couplings of the leptoquark to electrons, i.e. $y_{22} = y_{21}$ and $y_{32} = y_{31}$. This would also lead to signatures with different flavored dileptons which often have much stronger constraints. These constraints are examined in section III. In the flavour universal case, the strongest limits on leptoquark masses will come from $\mu \rightarrow e$ processes including $\mu \rightarrow e\gamma$ [18] and $\mu \rightarrow 3e$ [19] measurements. However, it might be possible that the effects of leptoquarks could be cancelled in loop-induced processes by the presence of other new particles. Studying direct leptoquark production at the LHC allows us to directly probe the lepton-universal case because the observed number of events in $\mu\mu$, ee and μe channels will be correlated.

Our paper is structured as follows: we start by listing out the model Lagrangian and the resulting Wilson coefficients for C_9 in section II. We then examine the current LHC constraints in various search channels in section III and expected detection prospects of future colliders are calculated in section IV.

II. LEPTOQUARK MODELS

Leptoquarks are bosons which carry both $SU(2)_L$ and colour $SU(3)$ charges and therefore couple to both leptons and quarks. Given that we need to get the right contribution to $C_9^{\mu^+\mu^-}$, this corresponds to a leptoquark that at a minimum couples to muons and to b and s quarks. There are three known leptoquark models that give the right kind of contribution [12–14, 20], which we describe below. We use the standard names for the fields, viz. S_3 , R_2 and U_1 and the numbers in brackets that follow correspond to (n-plet of $SU(3)$, n-plet of $SU(2)$, $U(1)_Y$ hypercharge). Of these, S_3 and R_2 are scalar fields and U_1 is a vector field.

A. Scalar Leptoquark $S_3(\bar{3}, 3, 1/3)$

The first leptoquark model we consider is $S_3(\bar{3}, 3, 1/3)$ which is a $SU(2)_L$ triplet of scalar leptoquark states with hypercharge $1/3$. S_3 is the only scalar leptoquark model that can simultaneously predict $R_{K^*}^{exp} < R_{K^*}^{SM}$ and $R_{K^*}^{exp} < R_{K^*}^{SM}$ at tree level [21–24]. The Lagrangian for the S_3 model is

$$\mathcal{L}_{S_3} = y_L^{ij} \bar{Q}_i^C i\tau_2 (\tau_k S_3^k) L_j + h.c., \quad (\text{II.1})$$

where Q_i and L_j are $SU(2)_L$ doublet fermion fields corresponding to quarks and leptons of the i^{th} (j^{th}) generation respectively, τ_k are the generators of $SU(2)_L$, and y_L^{ij} stands for a Yukawa matrix for the left-handed fermions. The three triplet component states of S_3 carry charges $Q = -2/3, 1/3$ and $4/3$ respectively. Expanding out the $SU(2)_L$ components and referring to the leptoquarks as S_3^Q , we get

$$\begin{aligned} \mathcal{L}_{S_3} = & -y_L^{ij} \bar{d}_{Li}^C \nu_{Lj} S_3^{1/3} - \sqrt{2} y_L^{ij} \bar{d}_{Li}^C \ell_{Lj} S_3^{4/3} \\ & + \sqrt{2} (V^* y_L)^{ij} \bar{u}_{Li}^C \nu_{Lj} S_3^{-2/3} - (V^* y_L)^{ij} \bar{u}_{Li}^C \ell_{Lj} S_3^{1/3} + h.c., \end{aligned} \quad (\text{II.2})$$

of which only the $\bar{d}_{Li}^C \ell_{Lj} S_3^{4/3}$ term contributes to O_9 . One can extract the Wilson coefficients for the $b \rightarrow sl^- l^+$ decay [12–14, 20],

$$C_9^{\ell_1 \ell_2} = -C_{10}^{\ell_1 \ell_2} = \frac{\pi v^2}{V_{tb} V_{ts}^* \alpha_{em}} \frac{y_L^{b\ell_1} (y_L^{s\ell_2})^*}{m_{S_3}^2}, \quad (\text{II.3})$$

B. Scalar Leptoquark $R_2(3, 2, 7/6)$

The second case we consider is a weak doublet of scalar leptoquarks with hypercharge $Y = 7/6$, i.e. $R_2(3, 2, 7/6)$. [25] The most general Lagrangian describing the Yukawa interactions with R_2 can be written as,

$$\mathcal{L}_{R_2} = y_R^{ij} \bar{Q}_i l_{R_j} R_2 - y_L^{ij} \bar{u}_{R_i} R_2 i\tau_2 L_j + h.c., \quad (\text{II.4})$$

where y_L and y_R are the Yukawa matrices corresponding to left- and right-handed lepton fields respectively. In terms of the components with R_2^Q denoting each leptoquark state with charge Q , the Lagrangian can be written as

$$\begin{aligned} \mathcal{L}_{R_2} = & (V y_R)^{ij} \bar{u}_{L_i} \ell_{R_j} R_2^{5/3} + (y_R)^{ij} \bar{d}_{L_i} \ell_{R_j} R_2^{2/3} \\ & + (y_L)^{ij} \bar{u}_{R_i} \nu_{L_j} R_2^{2/3} - (y_L)^{ij} \bar{u}_{R_i} \ell_{L_j} R_2^{5/3} + h.c. \end{aligned} \quad (\text{II.5})$$

The tree-level contribution to the Wilson coefficients C_9 through the term $(y_R)^{ij} \bar{d}_{L_i} \ell_{R_j} R_2^{2/3}$ amounts to

$$C_9^{\ell_1 \ell_2} = C_{10}^{\ell_1 \ell_2} = -\frac{\pi v^2}{2V_{tb}V_{ts}^* \alpha_{em}} \frac{y_R^{s\ell_1} (y_R^{b\ell_2})^*}{m_{R_2}^2}, \quad (\text{II.6})$$

C. Vector Leptoquark $U_1(3, 1, 2/3)$

Finally, we describe the only vector leptoquark model considered in this paper, mainly because it has been the only model that could simultaneously explain both charged current and neutral current anomalies [12]. We consider the $U_1(3, 1, 2/3)$ model which gives a single leptoquark state with charge $2/3$. The most general Lagrangian consistent with the SM gauge symmetry allows couplings to both left-handed and right-handed fermions, namely

$$\mathcal{L}_{U_1} = \beta_L^{ij} \bar{Q}_i \gamma_\mu L_j U_1^\mu + \beta_R^{ij} \bar{d}_{R_i} \gamma_\mu \ell_{R_j} U_1^\mu + h.c., \quad (\text{II.7})$$

with couplings β_L^{ij} and β_R^{ij} . The contributions to the left-handed couplings to the effective Lagrangian amount to

$$C_9^{\ell_1 \ell_2} = -C_{10}^{\ell_1 \ell_2} = -\frac{\pi v^2}{V_{tb}V_{ts}^* \alpha_{em}} \frac{\beta_L^{s\ell_1} (\beta_L^{b\ell_2})^*}{m_{U_1}^2}, \quad (\text{II.8})$$

III. LHC LIMITS

Our goal is to use published LHC data to simultaneously constrain the mass and Yukawa couplings of the leptoquarks. The Wilson coefficient C_9 depends on three parameters roughly as

$$C_9^{\ell,\ell} \sim \left(\frac{y_{2\ell} y_{3\ell}}{M} \right)^2$$

where y_{ij} refers to the leptoquark coupling between the i^{th} generation of quark and j^{th} generation lepton. This corresponds to Yukawa couplings for S_3 and R_2 models and the gauge coupling for the U_1 model. Therefore, its possible to find a surface in the 3D parameter space that gives the required value of C_9 . However, most LHC search constraints are in principle only 2D — one coupling that determines the cross section of the final state and one mass. We, therefore, have several options in which to view the full constraints.

Let us start with $\ell = 2$ (i.e. μ) which contributes to $C_9^{\mu\mu}$. To be able to independently constrain the two Yukawa couplings y_{22} and y_{32} , we study three different cases — first setting only y_{22} non-zero (see figure 1, second setting only y_{32} non-zero (see figure 4) and third, setting both equal (see figure 5). Using the upper limits from the non-resonant dimuon search gives us an upper limit on y_{22} at each mass value. It is possible to also determine the minimal allowed value of y_{22} that is consistent with C_9 by requiring $y_{32} \leq 1$.

Since the latest LHCb data seem to indicate that electrons and muons have identical behaviour, we can indeed also do a similar exercise with y_{21} and y_{31} which would contribute to C_9^{ee} . Besides these, non-zero values of all four couplings (or even a single electron and a single muon coupling) — y_{21} , y_{31} , y_{22} and y_{32} can give signatures that have differently flavoured leptons in the final state, but without missing energy and therefore with no SM background.

It should be noted that in the case where a single leptoquark state can couple to both electrons and muons, the strongest constraints on couplings and mass of course come from low energy processes in the $\mu \rightarrow e$ sector [18, 19, 26]. However, it can still be an interesting exercise to directly probe the case where both y_{k1} and y_{k2} are non-zero. As we see in figure 2, this case is strongly constrained by the LHC, with the U_1 model likely to be ruled out already with full run-2 data of 139 fb^{-1} .

Since multiple leptoquark states come from the same multiplet, they have identical mass and switching on a single coupling allows the production of multiple states. For calculating

the LHC limits, we allow the production of all leptoquark states and select only that fraction that decays into the final state selected for by the analysis being reinterpreted. For example, in the S_3 case, if we look for pair production of leptoquark followed by decay of each into a muon and a jet by turning on $y_{22} \neq 0$ alone, we allow both the production of pairs of $S_3^{4/3} \rightarrow \bar{s}\mu^+$ as well as pairs of $S_3^{1/3} \rightarrow \bar{c}\mu^+$. Our limits, therefore, are not identical to the simplified model limits that the experimental analysis publishes by producing only one state at a time, with 100% branching fraction into a certain channel. Similarly, when looking at dilepton distributions, we take into account, with interference, all leptoquark states in the t-channel that are allowed by non-zero couplings.

A. Computational setup

Since we examine the limits from dilepton searches which have been presented in the form of upper limits on generator-level cross sections with fiducial cuts, our computational setup is much simplified. We generate events using `Madgraph5_amc@NLO` [27] with the required fiducial cuts and do not need to perform further detector simulation. This approach has been proven to work well [28] and reproduces expected limits. For the UV models, we use the scalar leptoquark models for S_3 and R_2 described in [29] and for the vector leptoquark model for the U_1 case, we use the model described in [30–32]. When more complicated functionality is required, we use Pythia8 [33] to shower, hadronize and apply the required kinematic cuts on events.

B. Limits from resonant and non-resonant dilepton searches

We re-interpreted both the dilepton resonance search with 139 fb^{-1} [34] and the non-resonant dilepton search at 139 fb^{-1} [35] from ATLAS. We find that the non-resonant search results in much stronger limits and we continue with this search for the rest of our study. The exclusive dilepton state can only be seen with a t-channel leptoquark exchange. It is possible to have a dilepton plus two jets from strong production of leptoquarks, however, this process does not depend on the leptoquark-fermion couplings and results in only a mass limit which we deal with in the next subsection. With the interference of SM Drell-Yan production of leptons with the t-channel leptoquark mediated production, one expects to

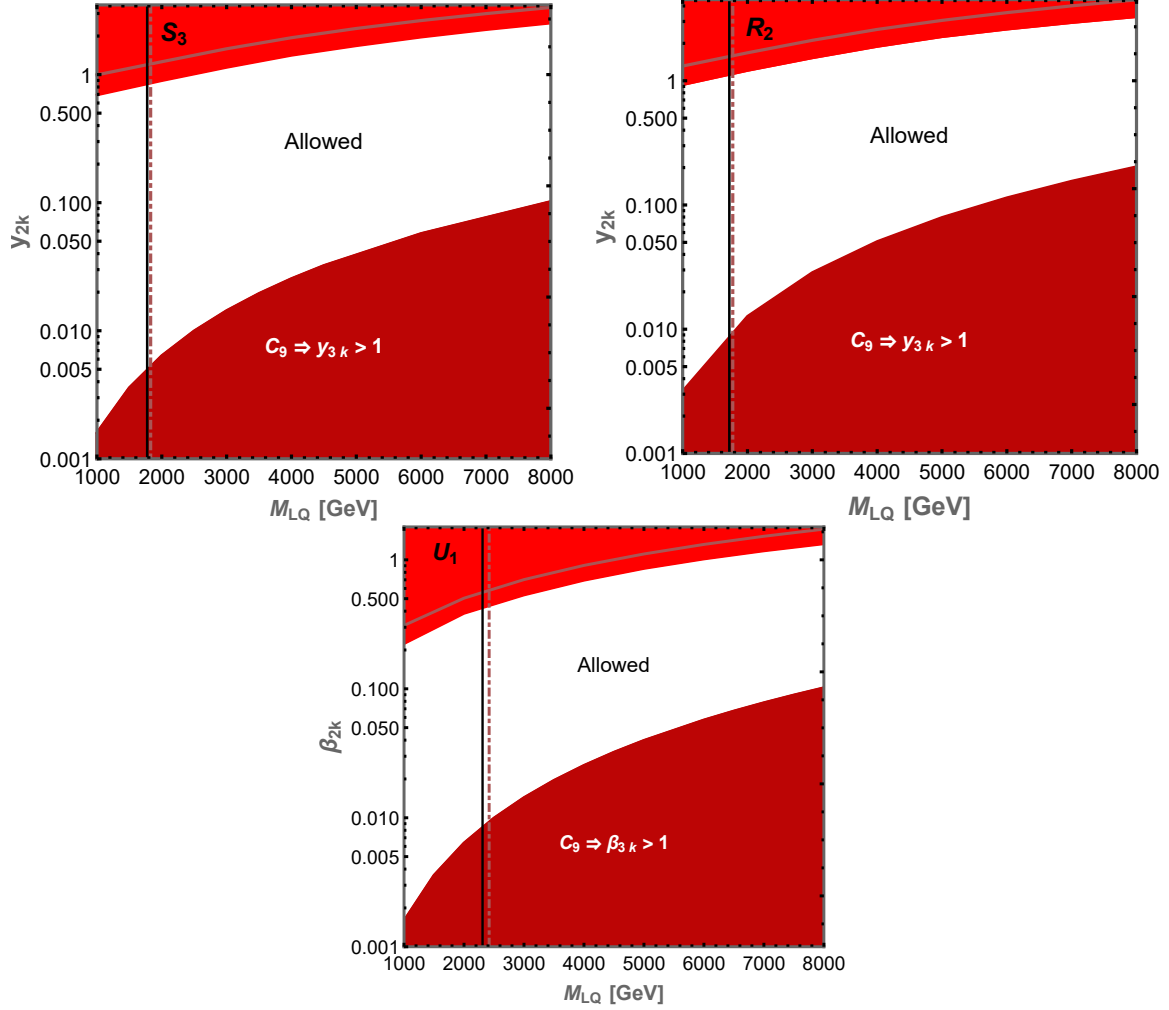


FIG. 1. Exclusion plots $y_{2\ell}$ versus Mass of leptoquark for the S_3 (top-left), R_2 (top-right) and U_1 models (bottom). The bright red regions at the top are disallowed from dimuon searches. The corresponding di-electron limit is the lighter line inside the red region. The solid regions at the bottom are from requiring perturbative couplings consistent with allowed C_9 . The vertical lines are mass limits from direct leptoquark pair production with the solid line corresponding to second generation leptons and the dotted corresponding to first generation. The limits correspond to 139 fb^{-1} data.

see a change in the shape of the dilepton invariant mass distribution $m_{\ell\ell}$ where $\ell = \mu$ or e .

We apply the limits from the ATLAS non-resonant dilepton search by generating events using `Madgraph5_amc@NLO` according to fiducial cuts listed in [35] and using the 95% upper limits for the most conservative signal region called the “ $\mu^+\mu^-$ constructive signal region” (or

analogously the e^+e^- constructive signal region). The constructive signal region corresponds to the case where you expect signal events above the EW expectation, which is similar to our case. The experimental analysis uses LO signal shape to model the expected number of events and we therefore also do not use any NLO corrections. The upper limits are provided on the additional cross section above the expected SM Electro-Weak (EW) prediction in the cumulative signal region where $m_{\mu^+\mu^-} \geq 2070$ GeV (or $m_{e^+e^-} \geq 2200$ GeV).

As expected, the effect of having heavy new leptoquarks in t-channel dies down when either the leptoquark mass is too high or the Yukawa coupling is too small. To account for the interference correctly, we use the difference of the cross-section $pp \rightarrow \ell^+\ell^-$ with both leptoquark and EW bosons, and with only EW gauge bosons as our new physics contribution. The result is an excluded region near high Yukawa coupling values, with a larger range ruled out for smaller leptoquark masses. This is shown as a bright red region in figure 1. The highest allowed value of y_{2k} is referred to as $y_{2k \text{ max}}$ and can be used to further restrict what values of y_{3k} are consistent with C_9 .

Currently, there is one different flavour dilepton search [36] performed at 13 TeV, but with only 3.2 fb data analysed. Aside from cuts on p_T of 65 and 50 GeV on electrons and muons respectively, there are requirements that missing energy be less than 25 GeV and $m_T < 50$ GeV to remove contamination from W-boson production which we apply using Pythia 8.3 [33]. The expected background for $m_{e\mu} > 2$ TeV is 0.02 ± 0.02 . They see one event and interpreting it as a statistical fluctuation, set a limit on new physics cross section. We extrapolate the expected limits from this search at 139 fb^{-1} . The limits on the $e\mu$ case for the U_1 model can be seen in figure 2. The expected background at 139 fb^{-1} is 2.78 events, resulting in an expected 95% upper limit of 0.0185 fb on production cross section times branching. As can be seen, the U_1 model should be completely ruled out with 139 fb^{-1} data. For results in the $e\mu$ channel for S_3 and R_2 models, refer to appendix C.

C. Limits from leptoquark-pair production

Direct limits on the mass of the leptoquark based on strong pair-production mode followed by the decay of each leptoquark into a lepton and a jet are presented in [37]. The limits are also presented on generator-level cross-section times branching fraction and can be applied directly to our model. The resulting limit is shown as a solid black vertical line. Since there

is no significant improvement in the limit from b-tagging, we use the general lepton+jet limits in all cases. When only y_{k2} is non-zero, i.e. the leptoquark decays to a muon and a jet, we obtain a mass limit for S_3 leptoquark at 1774 GeV, for the R_2 leptoquark at 1720 GeV and the U_1 leptoquark at 2309 GeV. For the case where the leptoquark decays into electron alone, we get a mass limit for S_3 leptoquark at 1828 GeV, for the R_2 leptoquark at 1773 GeV and the U_1 leptoquark at 2419 GeV.

There is no direct limit on the case with an $e\mu$ final state in the published search, which if it existed, would give a far better exclusion simply because there is no irreducible SM background and the dominant background would be from mis-identification of leptons.

D. Missing search: top FCNC decay

Given the need for non-zero leptoquark coupling to the third generation of quarks, this also implies a coupling between the top quark and second generation leptons for both the S_3 and U_1 models. In the R_2 case, the coupling is either CKM suppressed (in the case of left-handed) or entirely independent and therefore set to zero (in the right-handed case). It would therefore be possible to search directly for FCNC top decay via $t \rightarrow c\mu\mu$.

Currently, there are no searches for $t \rightarrow c\mu^+\mu^-$ except for a $t \rightarrow cZ$ search which requires the dimuon mass to be within 15 GeV of the Z mass [38] and therefore is not directly applicable to our model. A similar measurement from CMS [39] is available from the 8 TeV run.

The main background for a $t \rightarrow c\mu^+\mu^-$ search is from the SM production of $t\bar{t}\mu^+\mu^-$ via an off-shell Z or γ produced in association with $t\bar{t}$. To remove contamination from on-shell Z, we apply a cut instead $M_{\ell\ell} > 105$ which is outside the Z-mass window selected for by the $t \rightarrow cZ$ searches. Assuming the identification acceptances do not change, we can estimate the background for our proposed search using the data driven estimate presented in [38] (denoted by $\sigma_{BG,ATLAS}$). Since we have identical SM production modes for $t\bar{t}Z$ and $t\bar{t}\mu^+\mu^-$, we assume that the generator level transfer factor between these processes is transmitted all the way to the final selection. The kinematic effect of changing the $m_{\ell\ell}$ cut from $|M_{\ell\ell} - M_Z| < 15$ to $M_{\ell\ell} > 105$ can be estimated at generator level and is encapsulated in a single number $f_{\ell\ell}$. Also, we assume that the enhancement in production of $t\bar{t}Z$ in going

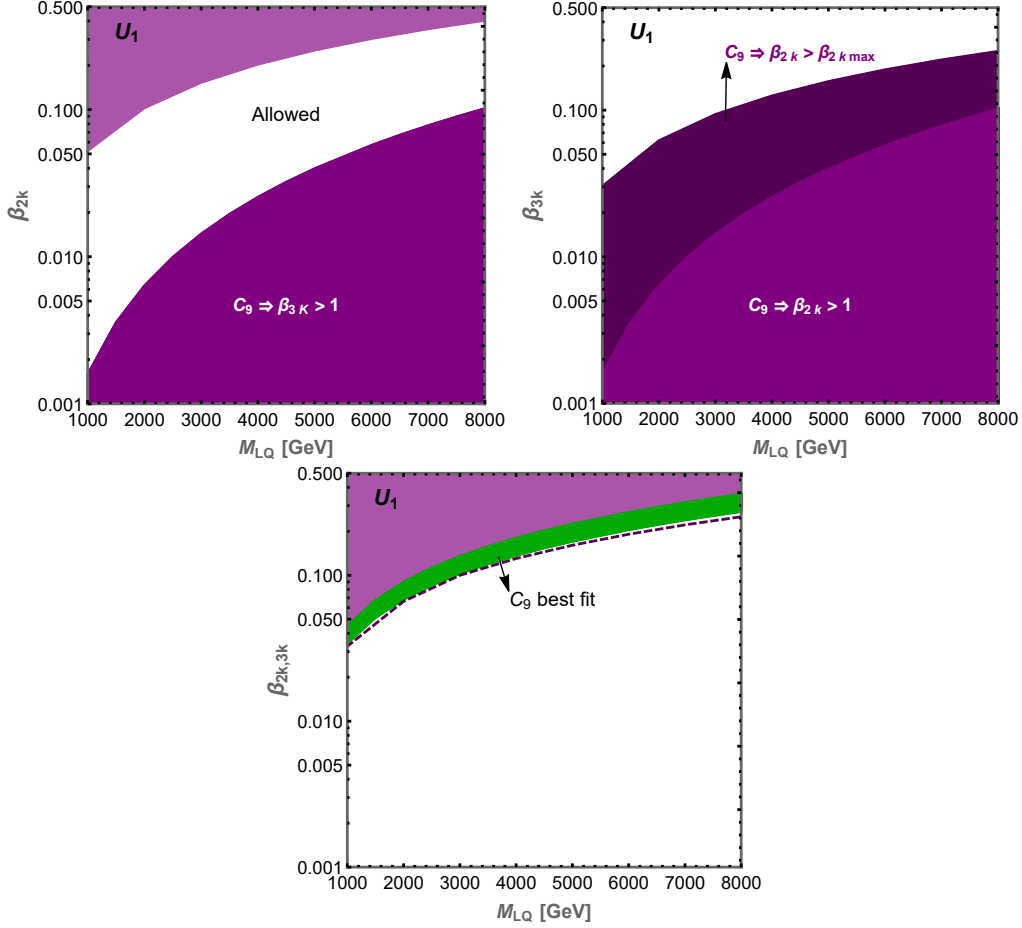


FIG. 2. Limits for the Leptoquark Couplings versus mass for the U_1 Model. The dilepton process, in this case, is $pp \rightarrow \mu e$ which does not exist in the SM. We, therefore, have strong limits even with 3.2 fb^{-1} data as published in [36]. The top-left panel shows limits on the coupling to second generation quarks with $y_{22} = y_{21}$, the top-right panel on the coupling to third generation quarks with $y_{32} = y_{31}$ and the bottom panel shows the case where all four couplings are equal. The green band shows the values corresponding to the best fit values of C_9 . The dotted line in this figure shows the expected limit after analysing full 139 fb^{-1} of run-2 data by ATLAS (only partial result is published so far). We see clearly that the universal scenario is likely already ruled out by run-2 data.

from 13 TeV to 13.6 TeV ($f_E = \frac{\sigma_{13.6}}{\sigma_{13}}$) remains the same also for $t\bar{t}\mu^+\mu^-$. Thus we have

$$\begin{aligned} \sigma_{BG}(\sqrt{s} = 13.6) &= \sigma_{BG,ATLAS} \\ &\times f_E \times f_{\ell\ell} \\ &\times \frac{\sigma(pp \rightarrow t\bar{t}\mu^+\mu^-; \sqrt{s} = 13)}{\sigma(pp \rightarrow t\bar{t}Z; \sqrt{s} = 13)} \end{aligned} \quad (\text{III.1})$$

Using this, and the expected background cross section from ATLAS, we calculate an expected background of 7 ± 2 events. Given that with the Z-window, the background is estimated at 119 ± 10 events, this would correspond to over an order of magnitude improvement in the sensitivity to FCNC branching fraction of the top quark.

IV. FUTURE PROSPECTS

The best-fit value of the Wilson coefficients for operators that explain the $b \rightarrow s$ anomalies suggests a high suppression scale. Using equations (II.6), (II.3) and (II.8), we find that the required scale for both couplings set to one is 16183 GeV for the R_2 case and 22887 GeV for the S_3 and U_1 cases. Naturally, resonantly producing a leptoquark of this mass scale is out of the question at the LHC. We, therefore, investigate both the expected reach of the LHC after the planned high-luminosity run and estimate a conservative reach for a muon collider with CM energy of 3 TeV [40–43]. To illustrate the highest sensitivity case, we choose $y_{22} = y_{32}$ for this calculation. This also allows us to make a comment on the ability of the collider to explore the entire parameter space of interest. A summary of the expected reach of future colliders can be seen in figure 3

A. LHC High-Lumi expected limits

Projections for the HL-LHC are made with the luminosity of 3000 fb^{-1} . From previous experience, we know that the improvements in limits scale with about the square root of luminosity. Using the expected number of signal and background events for the non-resonant dilepton search, we can probe effects of leptoquarks up to mass 5 TeV for the S_3 , 3 TeV for the R_2 and 9.5 TeV for the U_1 model. Conversely, we can probe coupling values as small as 0.4 for S_3 , 0.55 for R_2 and 0.15 for U_1 models respectively at 1 TeV leptoquark mass. For

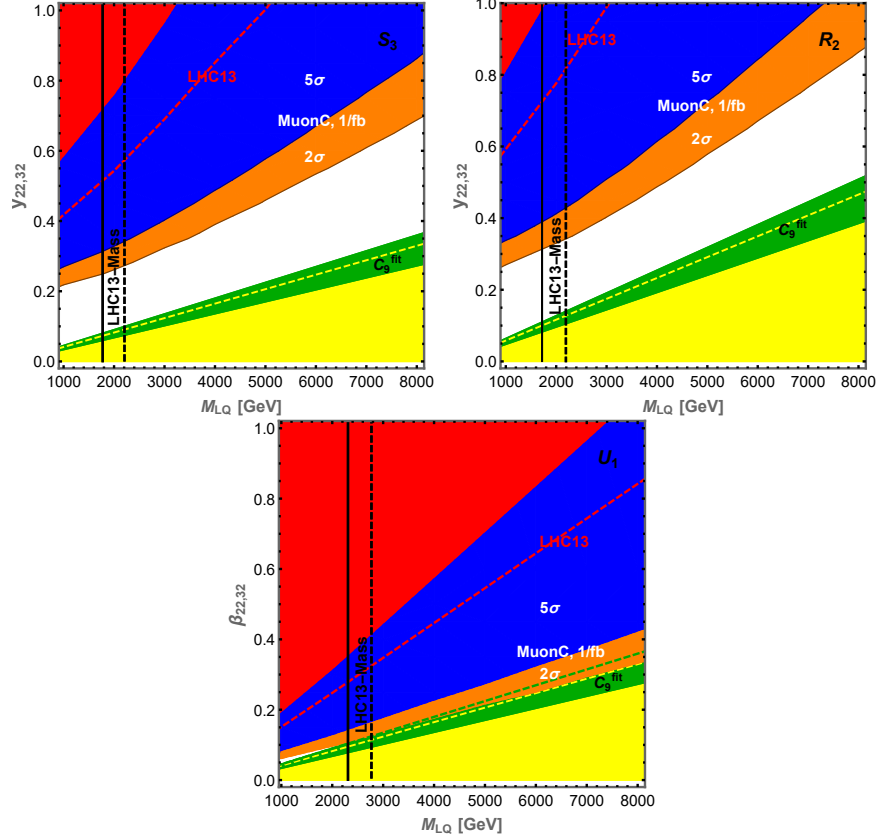


FIG. 3. Current and future reach in leptoquark coupling to muons with leptoquark mass for the S_3 Model (top-left), R_2 Model (top-right) and U_1 Model (bottom). The green region corresponds to the 1σ region given by global fit C_9 values in the model-dependent case whereas the yellow is the data-driven 1σ region ([7], also see table I). The solid red region is the current 139 fb^{-1} limits with the dotted red line the expected reach after 3 ab^{-1} at the HL-LHC. The solid and dotted vertical lines correspond to mass limits from pair production again corresponding to the 139 fb^{-1} and 3 ab^{-1} luminosity respectively. The blue region corresponds to the parameter space that can be discovered with a 5σ significance at a 3 TeV muon collider with 1 fb^{-1} whereas the orange region corresponds to the further region that can be probed at 95% confidence at the same collider. The U_1 model can be fully excluded with just 1 fb^{-1} data. The S_3 and R_2 models can also be fully probed with 6.5 fb^{-1} and 5 fb^{-1} respectively.

comparison, C_9 best fit predicts a minimum value of coupling at 0.04, 0.06 and 0.04 for the three models when we set both couplings equal.

The direct search limits from strong production are calculated in a similar way using the

published upper limits at 139/fb. We find that the HL-LHC can exclude leptoquark masses of 2.2 TeV for both the S_3 and R_2 case and 2.8 TeV for the U_1 case for the leptoquark decaying into a muon and a jet and 2.3 TeV for both the S_3 and R_2 case and 2.9 TeV for the U_1 case for the leptoquark decaying into an electron and a jet.

B. Reach of a Future Muon Collider

Estimating the reach of a future muon collider is more difficult since we do not currently have a detector configuration to be able to simulate a realistic analysis. However, taking lessons from the dilepton and dijet searches at the LHC, we know that a single-bin analysis with a high enough cut on the invariant mass provides a very reliable estimate of reach. We look at $\mu^+\mu^- \rightarrow jj$ as our signal. Obviously using b-tagging will be a further improvement that can pinpoint the underlying scenario. However, for this estimate, we just use untagged jets. Given that acceptance efficiencies of jets are expected to be similar for both signal and background events for a simple dijet search, we proceed with using just generator-level cross sections. A further advantage is the much reduced probability of extra initial state radiation jets from initial state muons (in sharp contrast to a pp machine).

The main background from the SM comes from s-channel photon or Z exchange. In the presence of the leptoquark, another Feynman diagram with a t-channel leptoquark exchange needs to be taken into account. We look only at events with $M_{jj} > 500$ GeV. The SM-only cross section at LO is 5.96×10^{-2} pb which corresponds to a statistical error of about 8 events at a luminosity of 1 fb^{-1} . Using this, we can calculate the parameter space corresponding to a 5σ discovery as well as regions that can be excluded at 2σ . They are shown in figure 3 as blue and orange regions respectively. In the U_1 case, we see that a muon collider is capable of excluding the entire viable parameter space with 1 fb^{-1} . To exclude the R_2 and S_3 models would need a luminosity of 6.5 fb^{-1} for S_3 and 5 fb^{-1} for R_2 .

V. SUMMARY AND CONCLUSIONS

We examine the limits from direct collider searches on leptoquark models that are capable of explaining the anomalous measurements in the decays of B-mesons. We focus on three specific models — two scalar leptoquark models S_3 and R_2 and one vector leptoquark model

U_1 . Aside from limits on the mass of the leptoquarks (which can be pair-produced by strong interactions), it is possible to also constrain the couplings to fermions by looking at changes to the shape of the dilepton mass spectrum. Reinterpreting full Run-2 limits from the pair production and non-resonant dilepton searches by ATLAS experiment, we find that current mass limits are 1.77 TeV, 1.72 TeV and 2.3 TeV respectively for the three models. We can expect to reach up to 2.2 TeV for S_3 and R_2 and 2.8 TeV for the U_1 respectively with the High-Luminosity LHC run.

Effects of leptoquarks with couplings to muons can potentially be probed in a muon collider. Since there has been considerable interest in a future muon collider recently, we also estimate what the reach of the proposed 3 TeV muon collider would be for the three models in question. We find that with very minimal assumptions, S_3 , R_2 and U_1 models show significant deviation in dijet distributions that can be observable for the entire range of interest with less than 6 fb^{-1} data for all three models.

ACKNOWLEDGEMENTS

ND is supported by the Ramanujan Fellowship grant SB/S2/RJN-070 from the Department of Science and Technology of the Government of India.

-
- [1] LHCb collaboration, *Test of lepton universality in $b \rightarrow s\ell^+\ell^-$ decays*, 2212.09152.
 - [2] LHCb collaboration, *Measurement of lepton universality parameters in $B^+ \rightarrow K^+\ell^+\ell^-$ and $B^0 \rightarrow K^{*0}\ell^+\ell^-$ decays*, 2212.09153.
 - [3] ATLAS collaboration, *Study of the rare decays of B_s^0 and B^0 mesons into muon pairs using data collected during 2015 and 2016 with the ATLAS detector*, *JHEP* **04** (2019) 098 [1812.03017].
 - [4] CMS collaboration, *Measurement of properties of $B_s^0 \rightarrow \mu^+\mu^-$ decays and search for $B^0 \rightarrow \mu^+\mu^-$ with the CMS experiment*, *JHEP* **04** (2020) 188 [1910.12127].
 - [5] LHCb collaboration, *Angular Analysis of the $B^+ \rightarrow K^{*+}\mu^+\mu^-$ Decay*, *Phys. Rev. Lett.* **126** (2021) 161802 [2012.13241].

- [6] N. Gubernari, M. Reboud, D. van Dyk and J. Virto, *Improved theory predictions and global analysis of exclusive $b \rightarrow s\mu^+\mu^-$ processes*, *JHEP* **09** (2022) 133 [2206.03797].
- [7] M. Ciuchini, M. Fedele, E. Franco, A. Paul, L. Silvestrini and M. Valli, *Constraints on Lepton Universality Violation from Rare B Decays*, 2212.10516.
- [8] M. Ciuchini, A. M. Coutinho, M. Fedele, E. Franco, A. Paul, L. Silvestrini et al., *New Physics in $b \rightarrow s\ell^+\ell^-$ confronts new data on Lepton Universality*, *Eur. Phys. J. C* **79** (2019) 719 [1903.09632].
- [9] M. Algueró, B. Capdevila, A. Crivellin, S. Descotes-Genon, P. Masjuan, J. Matias et al., *Emerging patterns of New Physics with and without Lepton Flavour Universal contributions*, *Eur. Phys. J. C* **79** (2019) 714 [1903.09578].
- [10] A. K. Alok, A. Dighe, S. Gangal and D. Kumar, *Continuing search for new physics in $b \rightarrow s\mu\mu$ decays: two operators at a time*, *JHEP* **06** (2019) 089 [1903.09617].
- [11] T. Hurth, F. Mahmoudi, D. M. Santos and S. Neshatpour, *More Indications for Lepton Nonuniversality in $b \rightarrow s\ell^+\ell^-$* , *Phys. Lett. B* **824** (2022) 136838 [2104.10058].
- [12] A. Angelescu, D. Bečirević, D. A. Faroughy and O. Sumensari, *Closing the window on single leptoquark solutions to the B-physics anomalies*, *JHEP* **10** (2018) 183 [1808.08179].
- [13] D. Bečirević, N. Košnik, O. Sumensari and R. Zukanovich Funchal, *Palatable Leptoquark Scenarios for Lepton Flavor Violation in Exclusive $b \rightarrow s\ell_1\ell_2$ modes*, *JHEP* **11** (2016) 035 [1608.07583].
- [14] S. Descotes-Genon, L. Hofer, J. Matias and J. Virto, *Global analysis of $b \rightarrow s\ell\ell$ anomalies*, *JHEP* **06** (2016) 092 [1510.04239].
- [15] C. Cornella, J. Fuentes-Martin and G. Isidori, *Revisiting the vector leptoquark explanation of the B-physics anomalies*, *JHEP* **07** (2019) 168 [1903.11517].
- [16] J. Aebischer, W. Altmannshofer, D. Guadagnoli, M. Reboud, P. Stangl and D. M. Straub, *B-decay discrepancies after Moriond 2019*, *Eur. Phys. J. C* **80** (2020) 252 [1903.10434].
- [17]
- [18] MEG collaboration, *New constraint on the existence of the $\mu^+ \rightarrow e^+\gamma$ decay*, *Phys. Rev. Lett.* **110** (2013) 201801 [1303.0754].
- [19] SINDRUM collaboration, *Search for the Decay $\mu^+ \rightarrow e^+ e^+ e^-$* , *Nucl. Phys. B* **299** (1988) 1.

- [20] A. Angelescu, D. Bečirević, D. A. Faroughy, F. Jaffredo and O. Sumensari, *Single leptoquark solutions to the B-physics anomalies*, *Phys. Rev. D* **104** (2021) 055017 [2103.12504].
- [21] I. Doršner, S. Fajfer, D. A. Faroughy and N. Košnik, *The role of the S_3 GUT leptoquark in flavor universality and collider searches*, *JHEP* **10** (2017) 188 [1706.07779].
- [22] G. Hiller and M. Schmaltz, *R_K and future $b \rightarrow s\ell\ell$ physics beyond the standard model opportunities*, *Phys. Rev. D* **90** (2014) 054014 [1408.1627].
- [23] G. Hiller and I. Nisandzic, *R_K and R_{K^*} beyond the standard model*, *Phys. Rev. D* **96** (2017) 035003 [1704.05444].
- [24] C. Hati, G. Kumar, J. Orloff and A. M. Teixeira, *Reconciling B-meson decay anomalies with neutrino masses, dark matter and constraints from flavour violation*, *JHEP* **11** (2018) 011 [1806.10146].
- [25]
- [26] SINDRUM II collaboration, *Test of lepton flavor conservation in $\mu \rightarrow e$ conversion on titanium*, *Phys. Lett. B* **317** (1993) 631.
- [27] J. Alwall, M. Herquet, F. Maltoni, O. Mattelaer and T. Stelzer, *MadGraph 5 : Going Beyond*, *JHEP* **06** (2011) 128 [1106.0522].
- [28] D. Bhatia, N. Desai and A. Dighe, *Frugal $U(1)_X$ models with non-minimal flavor violation for $b \rightarrow s\ell\ell$ anomalies and neutrino mixing*, *JHEP* **04** (2022) 163 [2109.07093].
- [29] I. Doršner and A. Greljo, *Leptoquark toolbox for precision collider studies*, *JHEP* **05** (2018) 126 [1801.07641].
- [30] M. J. Baker, J. Fuentes-Martín, G. Isidori and M. König, *High- p_T signatures in vector-leptoquark models*, *Eur. Phys. J. C* **79** (2019) 334 [1901.10480].
- [31] L. Di Luzio, J. Fuentes-Martín, A. Greljo, M. Nardecchia and S. Renner, *Maximal Flavour Violation: a Cabibbo mechanism for leptoquarks*, *JHEP* **11** (2018) 081 [1808.00942].
- [32] C. Cornella, D. A. Faroughy, J. Fuentes-Martín, G. Isidori and M. Neubert, *Reading the footprints of the B-meson flavor anomalies*, *JHEP* **08** (2021) 050 [2103.16558].
- [33] C. Bierlich et al., *A comprehensive guide to the physics and usage of PYTHIA 8.3*, 2203.11601.
- [34] ATLAS collaboration, *Search for high-mass dilepton resonances using 139 fb^{-1} of pp collision data collected at $\sqrt{s} = 13 \text{ TeV}$ with the ATLAS detector*, *Phys. Lett. B* **796** (2019) 68 [1903.06248].

- [35] ATLAS collaboration, *Search for new non-resonant phenomena in high-mass dilepton final states with the ATLAS detector*, *JHEP* **11** (2020) 005 [2006.12946].
- [36] ATLAS collaboration, *Search for new phenomena in different-flavour high-mass dilepton final states in pp collisions at $\sqrt{s} = 13$ TeV with the ATLAS detector*, *Eur. Phys. J. C* **76** (2016) 541 [1607.08079].
- [37] ATLAS collaboration, *Search for pairs of scalar leptoquarks decaying into quarks and electrons or muons in $\sqrt{s} = 13$ TeV pp collisions with the ATLAS detector*, *JHEP* **10** (2020) 112 [2006.05872].
- [38] ATLAS collaboration, *Search for flavour-changing neutral current top-quark decays $t \rightarrow qZ$ in proton-proton collisions at $\sqrt{s} = 13$ TeV with the ATLAS detector*, *JHEP* **07** (2018) 176 [1803.09923].
- [39] CMS collaboration, *Search for associated production of a Z boson with a single top quark and for tZ flavour-changing interactions in pp collisions at $\sqrt{s} = 8$ TeV*, *JHEP* **07** (2017) 003 [1702.01404].
- [40] R. Palmer et al., *Muon collider design*, *Nucl. Phys. B Proc. Suppl.* **51** (1996) 61 [acc-phys/9604001].
- [41] R. B. Palmer, *Muon Colliders*, *Rev. Accel. Sci. Tech.* **7** (2014) 137.
- [42] C. M. Ankenbrandt et al., *Status of muon collider research and development and future plans*, *Phys. Rev. ST Accel. Beams* **2** (1999) 081001 [physics/9901022].
- [43] J. C. Gallardo et al., *$\mu^+\mu^-$ Collider: Feasibility Study*, *eConf* **C960625** (1996) R4.
- [44] M. Bordone, G. Isidori and A. Pattori, *On the Standard Model predictions for R_K and R_{K^*}* , *Eur. Phys. J. C* **76** (2016) 440 [1605.07633].
- [45] LHCb collaboration, *Test of lepton universality with $B^0 \rightarrow K^{*0}\ell^+\ell^-$ decays*, *JHEP* **08** (2017) 055 [1705.05802].
- [46] LHCb collaboration, *Test of lepton universality in beauty-quark decays*, *Nature Phys.* **18** (2022) 277 [2103.11769].
- [47] M. Beneke, C. Bobeth and R. Szafron, *Power-enhanced leading-logarithmic QED corrections to $B_q \rightarrow \mu^+\mu^-$* , *JHEP* **10** (2019) 232 [1908.07011].
- [48] LHCb collaboration, *Measurement of Form-Factor-Independent Observables in the Decay $B^0 \rightarrow K^{*0}\mu^+\mu^-$* , *Phys. Rev. Lett.* **111** (2013) 191801 [1308.1707].

- [49] LHCb collaboration, *Angular analysis of the $B^0 \rightarrow K^{*0} \mu^+ \mu^-$ decay using 3 fb^{-1} of integrated luminosity*, *JHEP* **02** (2016) 104 [[1512.04442](#)].
- [50] S. Descotes-Genon, T. Hurth, J. Matias and J. Virto, *Optimizing the basis of $B \rightarrow K^* l l$ observables in the full kinematic range*, *JHEP* **05** (2013) 137 [[1303.5794](#)].

Appendix A: Relevant observables in the $b \rightarrow s$ sector

Observable	Experiment	Theory (SM)
$R_{K_{[0.1,1.1]}}$	$0.994^{+0.090}_{-0.082}$ (stat) $^{+0.029}_{-0.027}$ (syst) [2022] [1, 2]	1.00 ± 0.01 [44])
$R_{K^*_{[0.1,1.1]}}$	$0.927^{+0.093}_{-0.087}$ (stat) $^{+0.036}_{-0.035}$ (syst) [2022] [1, 2]	1.00 ± 0.01 [44])
$R_{K_{[1.1,6]}}$	$0.949^{+0.042}_{-0.041}$ (stat) $^{+0.022}_{-0.022}$ (syst) [2022] [1, 2]	1.00 ± 0.01 [44])
$R_{K^*_{[1.1,6]}}$	$1.027^{+0.072}_{-0.068}$ (stat) $^{+0.027}_{-0.026}$ (syst) [2022] [1, 2]	1.00 ± 0.01 [44])
$R_{K^*}^{[0.045,1.1]}$	$0.66^{+0.11}_{-0.07} \pm 0.03$ [2021] [45]	0.906 ± 0.028 [44]
$R_{K^*}^{[1.1,6.0]}$	$0.69^{+0.11}_{-0.07} \pm 0.05$ [2021] [45]	1.00 ± 0.01 [44]
$R_K^{[1.1,6.0]}$	$0.846^{+0.042+0.013}_{-0.039-0.012}$ [2021] [46]	1.00 ± 0.01 [44]
$\mathcal{B}(B_s \rightarrow \mu^+ \mu^-)$	$(2.85^{+0.32}_{-0.31}) \times 10^{-9}$ [3, 4]	$(3.66 \pm 0.14) \times 10^{-9}$ [47])
P'_5 in $B \rightarrow K^{(*)} l^+ l^-$	[5, 48, 49]	[6, 50]

TABLE II. A summary of the most relevant experimental results and SM predictions for the observables in $b \rightarrow s$ sector.

Appendix B: Limits on leptoquark couplings to third generation quarks y_{3k} .

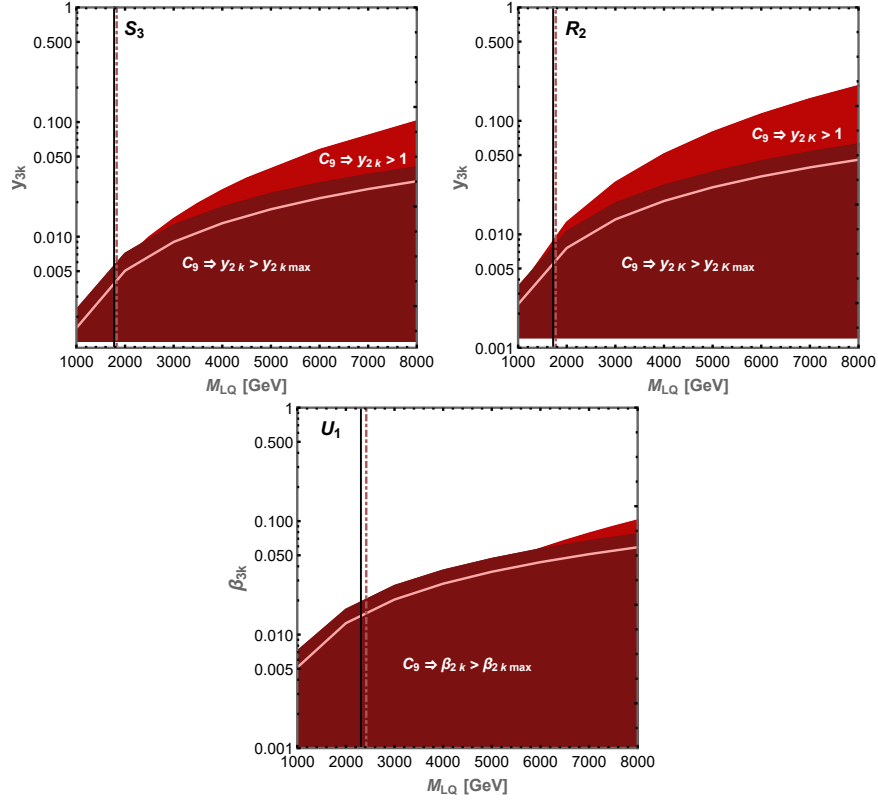


FIG. 4. Exclusion plots $y_{3\ell}$ versus Mass of leptoquark for the S_3 (top-left), R_2 (top-right) and U_1 models (bottom). The solid regions at the bottom are from requiring perturbative couplings consistent with allowed C_9 . The darker region is inconsistent with the observed upper limits on y_{2k} in figure 1. The vertical lines are mass limits from direct leptoquark pair production with the solid line corresponding to second generation leptons and the dotted corresponding to first generation. The limits correspond to 139 fb^{-1} data.

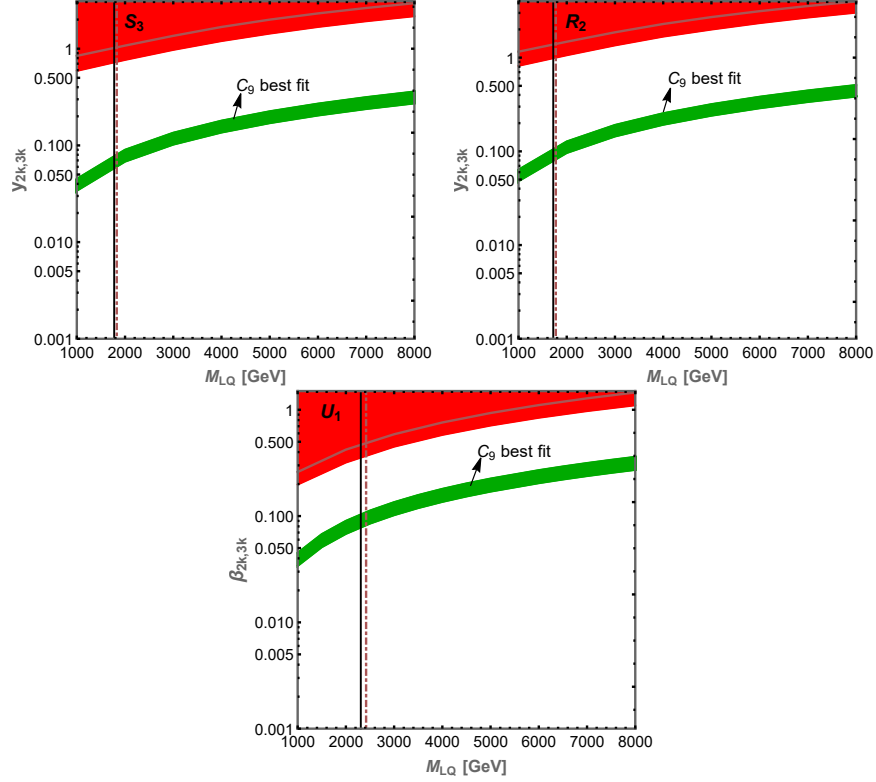


FIG. 5. Exclusion plots in the limited case of $y_{2\ell} = y_{3\ell}$ versus Mass of leptoquark for the S_3 (top-left), R_2 (top-right) and U_1 models (bottom). The solid red region at the top are limits from non-resonant dilepton searches in $\mu^+\mu^-$. The lighter lines inside this region correspond to subleading limits from the similar e^+e^- search. The vertical lines are mass limits from direct leptoquark pair production with the solid line corresponding to second generation leptons and the dotted corresponding to first generation. The limits correspond to 139 fb^{-1} data. The green band is the region that corresponds to the coefficient C_9 within one sigma of best fit to data.

Appendix C: Limits on S_3 and R_2 model parameters in the Lepton Flavour Universal case

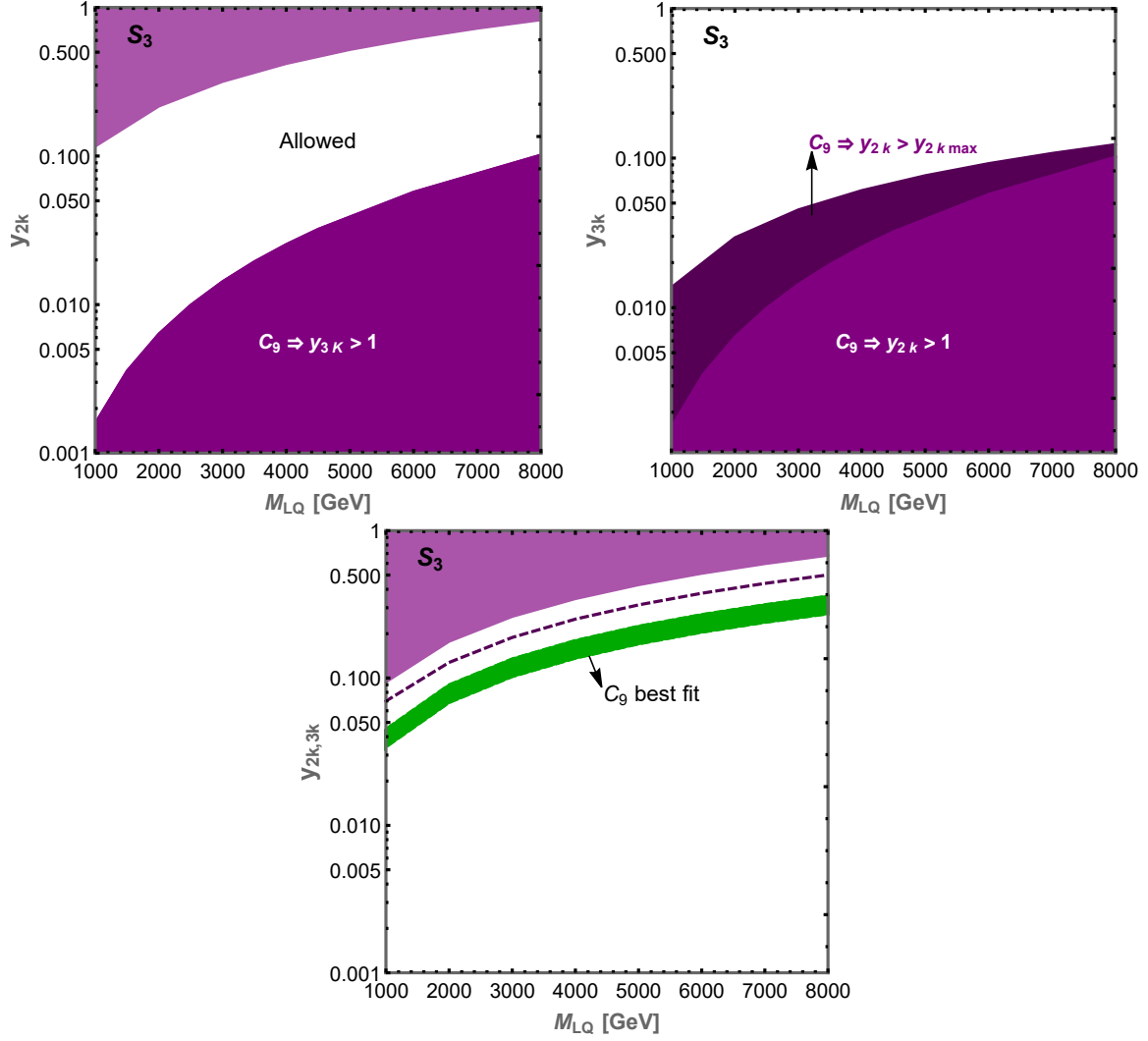


FIG. 6. Limits on the leptoquark couplings via the process $pp \rightarrow \mu e$ in the case of flavour universal couplings to electrons and muons for the S_3 Model.

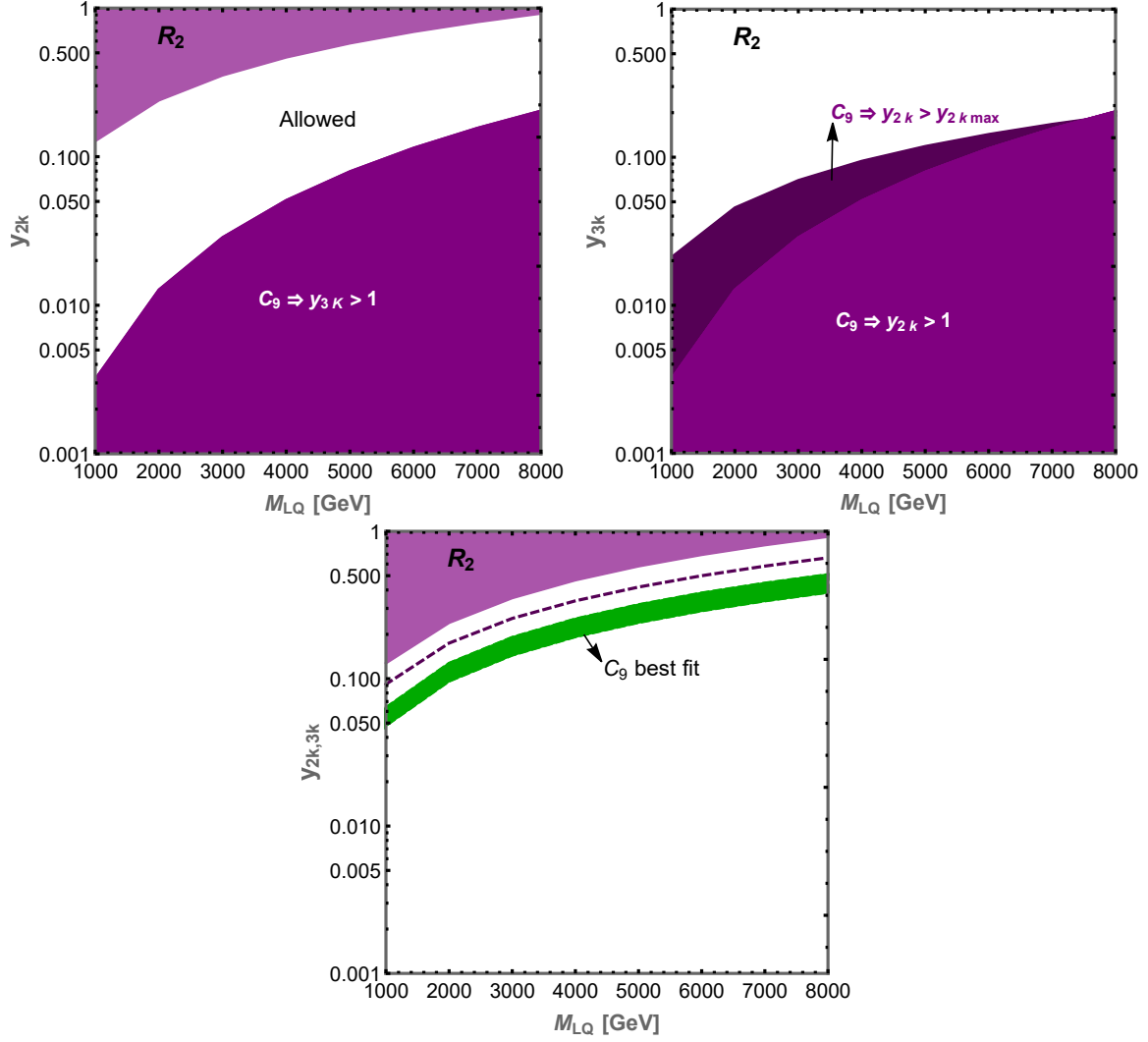


FIG. 7. Limits on the leptoquark couplings via the process $pp \rightarrow \mu e$ in the case of flavour universal couplings to electrons and muons for the R_2 Model.